

# Fibre-optics implementation of asymmetric phase-covariant quantum cloner

Lucie Bartůšková,<sup>1</sup> Miloslav Dušek,<sup>1</sup> Antonín Černocho,<sup>1,2</sup> Jan Soubusta,<sup>2</sup> and Jaromír Fiurášek<sup>1</sup>

<sup>1</sup>Department of Optics, Palacký University, 17. listopadu 50, 772 00 Olomouc, Czech Republic

<sup>2</sup>Joint Laboratory of Optics of Palacký University and Institute of Physics of Academy of Sciences of the Czech Republic, 17. listopadu 50A, 772 00 Olomouc, Czech Republic

(Dated: September 14, 2018)

We present the experimental realization of optimal symmetric and asymmetric phase-covariant  $1 \rightarrow 2$  cloning of qubit states using fiber optics. State of each qubit is encoded into a single photon which can propagate through two optical fibers. The operation of our device is based on one- and two-photon interference. We have demonstrated creation of two copies of any state of a qubit from the equator of the Bloch sphere. The measured fidelities of both copies are close to the theoretical values and they surpass the theoretical maximum obtainable with the universal cloner.

PACS numbers: 03.67.-a, 42.50.-p, 32.80.-t

The quantum no-cloning theorem [1] lies at the heart of quantum information theory. The apparently simple observation that perfect copying of unknown quantum states is impossible has profound consequences. On the fundamental side, it prevents superluminal communication with entangled states, thereby guaranteeing the peaceful coexistence of quantum mechanics and theory of relativity. On the practical side, this theorem is behind the security of the quantum key distribution schemes which rely on the fact that any attempt to measure or copy an unknown quantum state results in the disturbance of this state. Going beyond the no-cloning theorem, Bužek and Hillery in a seminal paper introduced the concept of the universal approximate quantum cloning machine that optimally approximates the forbidden transformation  $|\psi\rangle \rightarrow |\psi\rangle|\psi\rangle$  [2]. Today, optimal quantum cloners are known for many different cases and scenarios [3, 4]. During recent years, growing attention has been paid to the experimental implementation of quantum cloning machines and, in particular, optimal cloning of polarization states of single photons via stimulated parametric downconversion or via photon bunching on a beam splitter has been successfully demonstrated [5, 6, 7, 8, 9, 10].

Besides giving an insight into the fundamental limits on distribution of quantum information, the quantum cloning machines turned out to be very efficient eavesdropping attacks on the quantum key distribution protocols [11, 12, 13, 14]. In this context one is particularly interested in the *asymmetric* quantum cloners that produce two copies with different fidelities. In this way, the eavesdropper can control the trade-off between the information gained on a secret cryptographic key and the amount of noise added to the copy which is sent down the channel to the authorized receiver. While the theory of optimal asymmetric quantum copying machines is well established (see, e.g. the recent reviews [3, 4]), the experimental optical realization of such machines has received considerably less attention. This might be attributed to the fact that the asymmetric cloning operations exhibit

much less symmetry than the corresponding symmetric ones. To the best of our knowledge, asymmetric quantum cloning of single-photon states has been so far achieved only in a single experiment, where universal asymmetric copying of polarization states was performed by means of partial quantum teleportation [15].

In this Letter, we report on the experimental implementation of the optimal  $1 \rightarrow 2$  phase-covariant asymmetric cloning of photonic qubits represented by a single photon propagating in two single-mode optical fibers. The phase-covariant copying machine optimally clones all states on the equator of the Bloch sphere,  $|\psi\rangle = \frac{1}{\sqrt{2}}(|0\rangle + e^{i\phi}|1\rangle)$ . Our experiment is based on the interplay of single- and two-photon interference of two photons in an optical network built from optical fibers. This approach has several important technological advantages. First, the single-mode fibers guarantee very high interference visibility. Second, variable ratio couplers enable to easily change in a controlled way the cloning transformation and we are thus able to demonstrate the whole class of the optimal asymmetric cloners. In contrast to our previous experiment on the optimal symmetric phase-covariant cloning of polarization states of single photons [16], with the present fiber-based scheme [17] we are able to achieve fidelities exceeding the limit of optimal universal cloning machine. This is rather challenging because the fidelities of the optimal universal and phase-covariant cloners are very close. For instance, for a symmetric cloner we have  $F_{\text{univ}} = \frac{5}{6} \approx 0.833$  and  $F_{\text{pc}} = \frac{1}{2}(1 + \frac{1}{\sqrt{2}}) \approx 0.854$  so the fidelities differ only by 2.1%.

The optimal asymmetric phase-covariant cloning transformation requires only a single blank copy in addition to the input qubit to be cloned and reads [18],

$$\begin{aligned} |0\rangle &\rightarrow |00\rangle, \\ |1\rangle &\rightarrow \sqrt{q}|10\rangle + \sqrt{1-q}|01\rangle, \end{aligned} \quad (1)$$

where  $q \in [0, 1]$  characterizes the asymmetry of the clones and for the symmetric cloner  $q = \frac{1}{2}$ . The fidelities of the

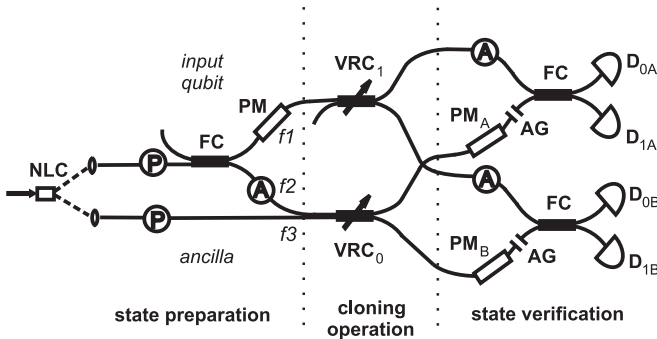


FIG. 1: Experimental setup. NLC denotes nonlinear crystal, P polarizers, FC fiber couplers, A attenuators, PM phase modulators, VRC variable-ratio couplers, AG adjustable air-gaps, D detectors.

two clones are given by

$$F_A = \frac{1}{2}(1 + \sqrt{q}), \quad F_B = \frac{1}{2}(1 + \sqrt{1 - q}). \quad (2)$$

In our scheme (see Fig. 1) each qubit is represented by a single photon which may propagate in two optical fibers and the basis states  $|0\rangle$  and  $|1\rangle$  correspond to the presence of the photon in the first or second fiber, respectively. The state of ancilla photon is initially  $|0\rangle$  while the signal photon can be prepared in an arbitrary state from the equator of the Bloch sphere. The two photons impinge on two unbalanced beam splitters (variable ratio couplers  $VRC_0$  and  $VRC_1$ ) with different splitting ratios. Let us suppose that real amplitude transmittances and reflectances of  $VRC_0$  and  $VRC_1$  are  $t_0$ ,  $r_0$  and  $t_1$ ,  $r_1$ , respectively. We use the notation  $R_j = r_j^2$  and  $T_j = t_j^2$  for the intensity reflectances and transmittances and  $R_j + T_j = 1$  for a lossless beam splitter. In the experiment, we accept only the events when there is a single photon detected in each output pair of fibers corresponding to the clone A and B, respectively. The cloning transformation is thus implemented conditionally, similarly to other optical cloning experiments. The resulting conditional transformation reads [19]

$$\begin{aligned} |0\rangle_{\text{Sig}}|0\rangle_{\text{Anc}} &\rightarrow (r_0^2 - t_0^2)|00\rangle, \\ |1\rangle_{\text{Sig}}|0\rangle_{\text{Anc}} &\rightarrow r_0 r_1 |10\rangle - t_0 t_1 |01\rangle. \end{aligned} \quad (3)$$

This becomes equivalent to the optimal cloning operation (1) up to a constant prefactor representing the probability amplitude of successful cloning, if the following equations hold,

$$r_0 r_1 = \sqrt{q}(r_0^2 - t_0^2), \quad t_0 t_1 = -\sqrt{1 - q}(r_0^2 - t_0^2).$$

Taking the square of the ratio of these two equations, we arrive at

$$R_1 = \frac{q(1 - R_0)}{q(1 - R_0) + (1 - q)R_0}, \quad (4)$$

and from the normalization  $T_1 + R_1 = 1$  we find after some algebra that  $R_0$  can be determined as a root of a cubic polynomial,

$$R_0(1 - R_0) + [R_0(2q - 1) - q](2R_0 - 1)^2 = 0. \quad (5)$$

The resulting reflectances are given in Tab. I for several values of the asymmetry parameter  $q$ . The equations have always two physically significant solutions that also require different signs of amplitude reflectances and transmittances. We have always selected the “less unbalanced” splitting ratios as they are more convenient from the experimental point of view.

Our experimental setup is shown in Fig. 1. A pair of signal and ancilla photons is prepared by means of frequency-degenerate type-I spontaneous parametric down-conversion in a 10-mm-long  $\text{LiIO}_3$  nonlinear crystal pumped by a krypton-ion cw laser (413.1 nm), similarly as in our previous experiments [16, 17]. The signal photon is split by a fiber coupler FC into two fibers. The basis states of the signal qubit,  $|0\rangle$  and  $|1\rangle$ , correspond to the presence of a photon either in fiber  $f_2$  or  $f_1$ , respectively. The intensity ratio and phase difference between these two modes determine the input state of the signal qubit. Preparation of the state is affected by unequal losses in the two optical paths  $f_1$  and  $f_2$  which alter the effective splitting ratio of FC. This effective splitting ratio is measured with the help of a semiconductor laser and a PIN photodiode and the attenuator in mode  $f_2$  is adjusted in such a way that the setup is balanced and at the end of the state preparation block the signal photon is evenly split between  $f_1$  and  $f_2$ . Various equatorial qubit states  $\frac{1}{\sqrt{2}}(|0\rangle + e^{i\phi}|1\rangle)$  can be then prepared by changing only the voltage applied to the phase modulator PM which sets the relative phase  $\phi$ . The ancilla is in a fixed state  $|0\rangle$  which corresponds to a single photon propagating through the fiber  $f_3$ .

The cloning operation is realized by two variable-ratio couplers  $VRC_0$  and  $VRC_1$ .  $VRC_0$  forms the core of Hong-Ou-Mandel (HOM) interferometer [20]. For optimal cloning it is necessary to achieve precise time overlap of the two photons at  $VRC_0$  and match their polarizations. To accomplish these tasks the splitting ratio of  $VRC_0$  is set to 50:50. We typically reach visibilities of HOM dip around 98%. Then the  $VRC_0$  splitting ratio is changed to the required value depending on the asymmetry parameter  $q$ , c.f. Table I.

The two fiber-based Mach-Zehnder (MZ) interferometers are adjusted using only the signal beam from the nonlinear crystal, the ancilla beam is blocked. Detection rates at each detector are measured and used for the alignment of the setup. First the intensity transmittances of the whole arms of each MZ interferometer are balanced with the help of the attenuators in the “state verification” part of the setup, which compensates for the unequal losses caused by the splitting ratios of variable ratio couplers, the phase modulators, air-gaps and

Theory					Experiment	
$q$	$R_0$	$R_1$	$F_A$	$F_B$	$F_A$	$F_B$
0.5	0.789	0.211	0.854	0.854	$0.854 \pm 0.004$	$0.834 \pm 0.004$
0.6	0.801	0.271	0.887	0.816	$0.881 \pm 0.006$	$0.789 \pm 0.005$
0.7	0.817	0.344	0.918	0.774	$0.905 \pm 0.003$	$0.754 \pm 0.005$
0.8	0.838	0.436	0.947	0.724	$0.935 \pm 0.002$	$0.714 \pm 0.006$
0.9	0.872	0.570	0.974	0.658	$0.964 \pm 0.002$	$0.641 \pm 0.004$
1.0	1.000	1.000	1.000	0.500	—	—

TABLE I: Asymmetric phase covariant cloner. Table shows calculated reflectances of variable ratio couplers and theoretical and measured fidelities for different parameters of asymmetry  $q$ . For  $q < 0.5$  the clones are just interchanged. Error intervals represent statistical errors.

other factors. Visibilities are maximized by adjusting zero path differences and aligning polarizations in the interferometers. In this setting visibilities above 97% are achieved. After this step we unbalance the MZ interferometers properly again: From the transmittances and reflectances of VRC<sub>0</sub> and VRC<sub>1</sub> used in the experiment and given in Table I we can determine what should be the detection rates for equal losses in the optical paths from VRC<sub>0</sub> and VRC<sub>1</sub> to FC. So, we tune the attenuators until we reach the point where these optical-path losses are balanced. This ensures that each detection block performs projections onto the states on the equator of the Bloch sphere.

To reduce the effect of a phase drift between arms of each MZ interferometer caused by fluctuations of temperature and temperature gradients we apply both passive and active stabilization. The experimental setup is thermally isolated in a polystyrene box. After this precaution the phase drift in each MZ interferometer has the average value  $\pi/1000$  per second. Therefore the active stabilization of phase differences is repeatedly applied after each three-second measurement period [17]. Only one beam from the crystal is used for the active stabilization and the other one is blocked. In each stabilization cycle the values of the phase drifts are estimated and they are compensated by means of phase modulators PM<sub>A</sub> and PM<sub>B</sub>. In this way, both interferometers are stabilized simultaneously.

We have experimentally realized cloning operation for the five values of asymmetry parameter  $q$  shown in Tab. I. For each  $q$  related to given splitting ratios of the couplers VRC<sub>0</sub> and VRC<sub>1</sub>, various states from the equator of the Bloch sphere were cloned. Two detection blocks are used to measure simultaneously fidelities of both clones. Each block consists of an attenuator, a phase modulator, a 50:50 fiber coupler and two detectors (Perkin-Elmer single-photon counting modules employing silicon avalanche photodiodes with quantum efficiency  $\eta \approx 50\%$ ). The cloning is successful only if one photon passes to the modes of qubit A and the other

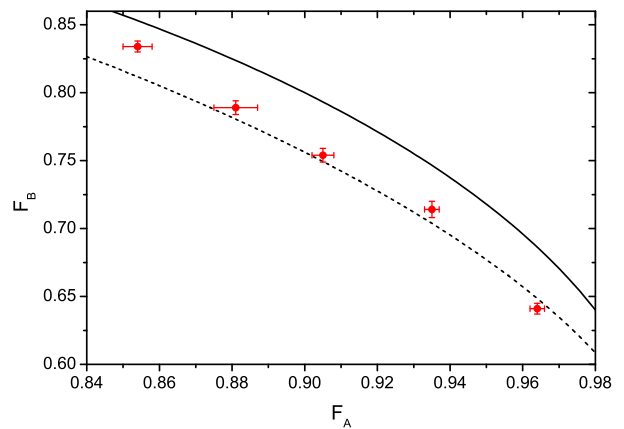


FIG. 2: Dependence of fidelity  $F_B$  on  $F_A$  for phase-covariant cloner with different asymmetries. Symbols denote experimental data, solid line represents theoretical prediction for optimal asymmetric phase-covariant cloner. Dashed line shows theoretical prediction for optimal asymmetric universal cloner.

one to the modes of qubit B. Hence coincidences between detectors  $D_{iA}$  and  $D_{jB}$  ( $i, j = 0, 1$ ) are counted. The signals from detectors are processed by coincidence electronics based on time-to-amplitude convertors and single-channel analyzers with a two-nanosecond coincidence window.

The measurement basis for each clone consists of the input signal state and the state orthogonal to it, which is guaranteed by the alignment procedure described above. Four coincidence rates  $C^{++}$ ,  $C^{--}$ ,  $C^{+-}$  and  $C^{-+}$  were measured. The first sign concerns clone A and the other one clone B; “+” means projection to the original signal state and “-” to its orthogonal complement. Fidelities of clones read

$$F_A = \frac{C^{++} + C^{+-}}{C^{++} + C^{--} + C^{+-} + C^{-+}},$$

$$F_B = \frac{C^{++} + C^{-+}}{C^{++} + C^{--} + C^{+-} + C^{-+}}. \quad (6)$$

Our results are summarized in Fig. 2 and in Tab. I. The fidelities for each value of asymmetry are averaged over all cloned signal states from the equator. Fig. 2 shows the fidelity of the second clone as a function of the fidelity of the first clone. One can see that there is a small systematic error – measured fidelities are always 1 – 2% lower than their theoretical values. This is caused by misalignments, limited precision of parameter setting and a phase drift in both MZ interferometers during the measurement period. However, the qualitative agreement between the theoretical curve for the optimal asymmetric phase-covariant cloner, determined by Eq. (2), and the measured data is very good. For comparison, the dashed line indicates the trade-off between the fidelities of the

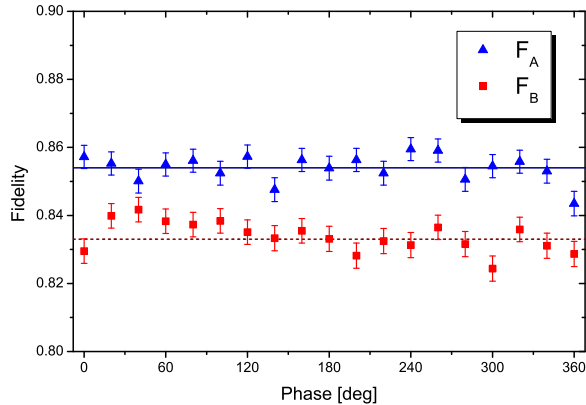


FIG. 3: Symmetric phase-covariant cloner. Fidelities  $F_A$  and  $F_B$  are plotted as functions of input-state phase  $\phi$ . Symbols denote experimental data, solid line represents theoretical prediction for the phase-covariant cloner, and the dashed line shows theoretical prediction for the universal cloner. Error bars represent statistical errors.

optimal universal asymmetric cloner [4],

$$F_A = 1 - \frac{(1-p)^2}{2(1-p+p^2)}, \quad F_B = 1 - \frac{p^2}{2(1-p+p^2)},$$

where  $p \in [0, 1]$ . Note that most of the experimental points lie in the area inaccessible by any universal cloning machine.

As an example, Fig. 3 shows data measured for the symmetric phase-covariant cloner ( $q = 0.5$ ). The splitting ratio of  $VRC_0$  was set to 21:79 whereas the splitting ratio of  $VRC_1$  to 79:21. The measurement was done for phases from  $0^\circ$  to  $360^\circ$  with a step of  $20^\circ$ . For each phase 40 three-second measurements were performed. Displayed fidelities are calculated from data measured simultaneously by all four detectors. The unequal detector efficiencies were compensated by proper rescaling of the measured coincidences. As expected, fidelities are nearly independent on phase. We can see that fidelities  $F_A$  and  $F_B$  of symmetric cloner are in fact slightly different due to imperfections of our setup. The splitting ratio of  $VRC_0$  was always set in such a way that the greater part of ancilla went to clone B. Therefore the visibility of HOM dip lower than 100% and the inaccuracy of position setting in HOM dip have stronger influence on fidelity  $F_B$  than  $F_A$ . However, the average of fidelities  $F_A$  and  $F_B$  overcomes the bound for universal cloner.

Because none of the output fiber couplers of MZ interferometers is precisely 50:50 the visibility of single photon interference cannot be perfect at both output ports of the coupler [21]. Therefore we have also measured all four coincidence rates sequentially at only one pair of detectors using proper phase shifts at phase modulators  $PM_A$  and  $PM_B$ . We had chosen the two detectors where the visibilities were maximized. Using only these

two detectors we have obtained fidelities (averaged over all phases):  $F_A = 0.840 \pm 0.009$ ,  $F_B = 0.850 \pm 0.009$ . In this kind of measurement no compensation for different detector efficiencies was needed.

In summary, we have demonstrated optimal symmetric and asymmetric phase-covariant cloning of single-photon states. Using fiber optics allowed us to reach very high visibilities and achieve fidelities exceeding the maximum obtainable by any universal cloning machine. Our implementation is compatible with fiber-based communication systems and represents a promising platform for realization of various protocols for quantum information processing.

This research was supported by the projects LC06007, 1M06002 and MSM6198959213 of the Ministry of Education of the Czech Republic and by the SECOQC project of the EC (IST-2002-506813).

- 
- [1] W.K. Wootters and W.H. Zurek, *Nature (London)* **299**, 802 (1982); D. Dieks, *Phys. Lett.* **92A**, 271 (1982).
  - [2] V. Bužek and M. Hillery, *Phys. Rev. A* **54**, 1844 (1996).
  - [3] V. Scarani, S. Iblisdir, N. Gisin, and A. Acín, *Rev. Mod. Phys.* **77**, 1225 (2005).
  - [4] N.J. Cerf and J. Fiurášek, In: *Progress in Optics*, vol. **49**, Ed. E. Wolf (Elsevier, 2006), p. 455.
  - [5] A. Lamas-Linares, C. Simon, J.C. Howell, and D. Bouwmeester, *Science* **296**, 712 (2002).
  - [6] F. De Martini, D. Pelliccia, and F. Sciarrino, *Phys. Rev. Lett.* **92**, 067901 (2004).
  - [7] M. Ricci, F. Sciarrino, C. Sias, and F. De Martini *Phys. Rev. Lett.* **92**, 047901 (2004).
  - [8] W.T. M. Irvine, A. Lamas-Linares, M. J. A. de Dood, and D. Bouwmeester, *Phys. Rev. Lett.* **92**, 047902 (2004).
  - [9] I.A. Khan and J.C. Howell, *Phys. Rev. A* **70**, 010303 (2004).
  - [10] F. Sciarrino and F. De Martini, *Phys. Rev. A* **72**, 062313 (2005).
  - [11] C.A. Fuchs, N. Gisin, R. B. Griffiths, C.-S. Niu, and A. Peres, *Phys. Rev. A* **56**, 1163 (1997).
  - [12] N.J. Cerf, M. Bourennane, A. Karlsson, and N. Gisin, *Phys. Rev. Lett.* **88**, 127902 (2002).
  - [13] M. Dušek, N. Lütkenhaus, M. Hendrych, In: *Progress in Optics*, vol. **49**, Ed. E. Wolf (Elsevier, 2006), p. 381.
  - [14] D. Bruss and C. Macchiavello, *Phys. Rev. Lett.* **88**, 127901 (2002).
  - [15] Z. Zhao, A.-N. Zhang, X.-Q. Zhou, Y.-A. Chen, C.-Y. Lu, A. Karlsson, and J.-W. Pan, *Phys. Rev. Lett.* **95**, 030502 (2005).
  - [16] A. Černocho, L. Bartůšková, J. Soubusta, M. Ježek, J. Fiurášek, M. Dušek, *Phys. Rev. A* **74**, 042327 (2006).
  - [17] L. Bartůšková, A. Černocho, R. Filip, J. Fiurášek, J. Soubusta, M. Dušek, *Phys. Rev. A* **74**, 022325 (2006).
  - [18] C.-S. Niu and R.B. Griffiths, *Phys. Rev. A* **60**, 2764 (1999).
  - [19] J. Fiurášek, *Phys. Rev. A* **67**, 052314 (2003).
  - [20] C.K. Hong, Z.Y. Ou, and L. Mandel, *Phys. Rev. Lett.* **59**, 2044 (1987).
  - [21] M. Hendrych, M. Dušek, O. Haderka, *Acta Physica Slovaca* **46**, 393 (1996).